

# Effect of Dopant ZnO Concentrations on Structural and Magnetic Properties of $\text{ZnMnO}_{3\pm\delta}$ Nanocrystalline

Geeta<sup>1</sup>, Sunita Dahiya<sup>2</sup>, Rajesh Sharma<sup>3\*</sup>

<sup>1</sup>Research Scholar, Baba Mastnath University, Rohtak-124001, India

<sup>2</sup>Faculty in Physics, Baba Mastnath University, Rohtak-124001, India

<sup>3</sup>Faculty in Physics, MNS Govt. College, Bhiwani - 127021, India

\*Corresponding Author- rkkaushik06@gmail.com

---

## ABSTRACT

The property of material changes with increase of surface atoms and especially proved contrasting behavior at the scale of nanometer. Among other metal Oxides Manganese Oxide ( $\text{MnO}_2$ ) have knee applications in the field of liquid crystal displays, high-temperature resistant materials, corrosive resistant materials, green pigment etc. The  $\text{MnO}_2$  have advance applications in the area of MRI and alloy formations. In present work, the ZnO doped  $\text{MnO}_2$  were synthesized by the Micro-wave irradiated chemical co-precipitation advance synthesis techniques. The ignited stuffs at  $600^\circ\text{C}/2\text{hrs}$  of various concentrations were characterized by the use of VSM, XRD, SEM, FTIR and the ionic TEM tools. The XRD results reveals that the grain size of newly calcined nanocomposites rises with rise of ZnO concentration 5%, 10% and 20% and may be due to larger radii of  $\text{Zn}^{2+}$  (Zinc ion) than Manganese. The FTIR Spectra of the ignited nano stuffs of ZnO doped  $\text{MnO}_2$  containing were found at wave number position sharp alps(peaks) inspected at  $483\text{ cm}^{-1}$  was due to Zn-O-Zn formation and  $466\text{ cm}^{-1}$ ,  $605\text{ cm}^{-1}$  were due to Mn-O-Mn vibration of Manganese Oxide molecules. The Perusal of TEM images exhibit that the size of all ignited ZnO doped  $\text{MnO}_2$  nanoparticulates lies in a confine of 31 nm to 42 nm and the intermediate fleck size is observed as 34 nm. The Perusal of scanning of sample through FESEM image is exhibiting that the flecks in the formation, cluttered in style and 2D in shape.

**Keywords:** Manganese Oxide nanocrystalline, XRD, FESEM, FTIR, TEM and VSM etc

---

## INTRODUCTION

Nanoscience focuses on understanding and manipulating materials at an extremely small scale, typically between one and one hundred nanometers. At this nanoscale, particles and materials exhibit unique properties that differ significantly from their larger counterparts. These properties include a high surface-to-volume ratio, which enhances their reactivity and interaction with other substances. Additionally, nanoparticles display distinct electrical and optical characteristics due to quantum confinement and photonic band gaps. Nanoparticles, often referred to as nano-stuffs, are small particles that fall within this nanoscale range. Their small size allows them to bridge the gap between bulk materials and individual molecules, giving them special significance in scientific research and technological applications.

Scientists are particularly interested in nanoparticles because they offer numerous advantages across various fields. For instance, their large surface-to-volume ratio makes them highly efficient catalysts in chemical reactions. In electronics, their distinct electrical properties can be harnessed to create smaller, more powerful devices. The optical properties of nanoparticles are utilized in developing advanced imaging techniques and medical diagnostics. Researchers explore these tiny materials to develop innovative solutions in medicine, electronics, energy, and environmental science. The potential applications of nanotechnology are vast and diverse, making it a rapidly evolving field with the promise to revolutionize many aspects of modern life. The authors of this work attempt to explain how change in dopant concentration altered structural and morphological features Manganese Oxide nanoparticulate with temperature.

### Synthesis Techniques

The chemicals and salts used in this investigation were high purity and acquired straight from a chemical unit. At the laboratory scale, no extra purification was performed.

To prepare a 1M solution of Manganese Nitrate ( $Mn(NO_3)_2 \cdot 4H_2O$ ) with a molecular weight of 251.01 g and appropriate amount of  $ZnCl_2 \cdot 5H_2O$  dissolve the material in 200 ml of distilled water. Slowly add ammonia ( $NH_3$ ) drop by drop to the resulting translucent solution until the pH reaches 9.0. Use a magnetic stirrer to continuously mix the solution for one hour at  $25^\circ C$ , ensuring it becomes homogeneous. Allow the resulting sludge to mature for at least 24 hours. After this period, filter the precipitates to separate the solids from the liquid. Wash the solid particles with ethanol and distilled water to remove any remaining by-products or impurities.

Remove the strained cake from the filter paper and dry it in a microwave oven set to  $125^\circ$  temperature for 2 sitting of 15 minutes. Next, place the dried material in a furnace and heat it at temperatures  $600^\circ C$ , for two hours, a process known as calcinations. The various calcined samples of  $Zn/MnO_2$  were transform to fine powder by using an pastel and agate mortar. Store the resulting fine powder in sealed airtight containers to keep it free from contamination. This powder is now ready for further analysis and use in various scientific and technological applications.

## CHARACTERIZATION OUTCOMES AND DISCUSSION

### X-ray Diffraction Investigations

The X-ray powder diffraction (XRD) patterns of Manganese Oxide nanocrystals, which were heated at different temperatures for 2 hours, were recorded and shown in Figure 1. The peak positions remained stable even after extended heating. To estimate the size of the crystals, the breadth ( $\beta$ ) of the most intense XRD peak was used in Debye-Scherrer's equation. This method allowed researchers to calculate the crystal sizes (D). The values of  $\beta$  and the corresponding crystal sizes (D) are displayed in Table 1. By using XRD data and Debye-Scherrer's equation, the size of the crystalline particles was systematically determined.

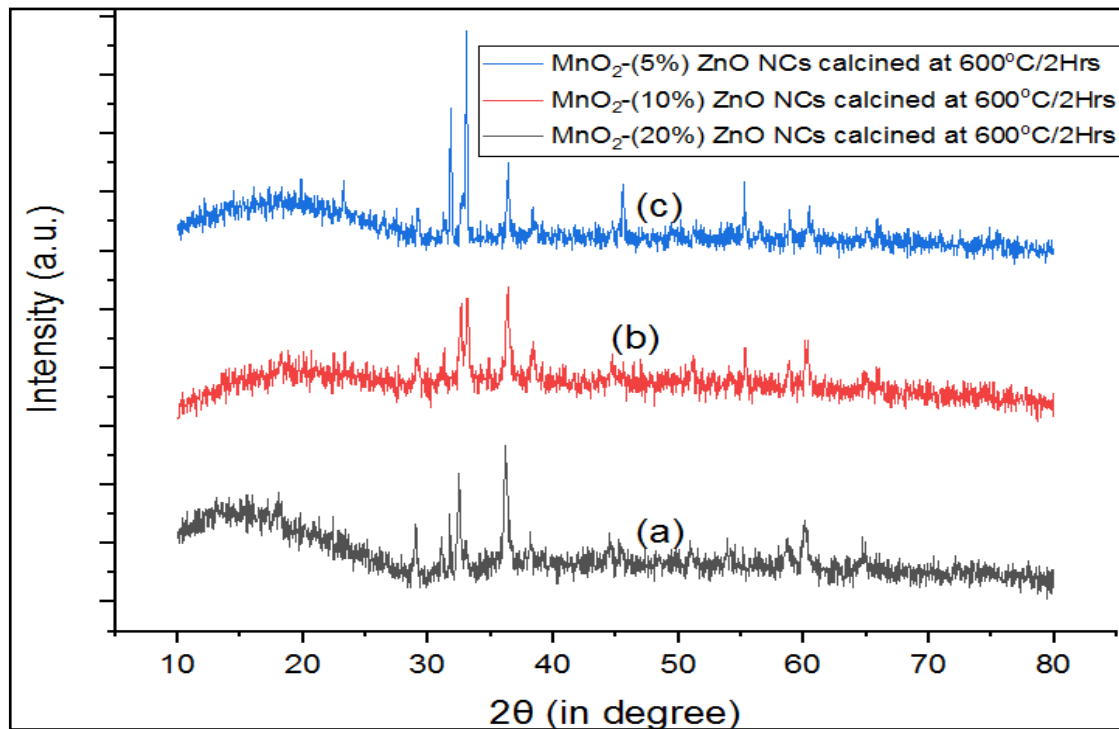


Figure-1. XRD graph of nanocrystalline calcined at  $600^\circ C/2hrs$  (a) 5%ZnO / $MnO_2$  (b) 10% ZnO / $MnO_2$  (b) 20% ZnO / $MnO_2$  NCs

The major Alps(peaks) for  $MnO_2$  nano-flecks with 5% dopant concentration at  $600^\circ C$  were reported to be at  $2\theta \sim 36.50^\circ$ ,  $33.17^\circ$ ,  $62.55^\circ$  and varied by the ICDD file no. 00-18-0802. The Alps(peaks) with 10% dopant concentration were outlined at  $36.58^\circ$ ,  $33.03^\circ$  and  $47.84^\circ$ ,  $47.37^\circ$ ,  $62.38^\circ$ .

The peaks with Zinc Oxide doped Manganese Oxide (20%) nano-sized stuff reported at  $2\theta \sim 34.50^\circ$ ,  $32.016^\circ$ ,  $47.83^\circ$ ,  $62.55^\circ$ , etc.

**Table-1. XRD facts of ZnO nano-flecks and ZnO doped MnO<sub>2</sub> nano-sized stuff ignited at 600<sup>0</sup>C with various dopant concentration**

Sr. No.	Title of specimen	period of calcinations	Spot of uttermost intense Alp (in degree)	Measure of FWHM or( $\beta$ ) (in radian)	Grain size
1.	ZnO(5%)/MnO <sub>2</sub>	2 hours	46.17	0.423	36.06 nm
2.	ZnO(10%)/MnO <sub>2</sub>	2 hours	46.03	0.436	34.17 nm
3.	ZnO(20%)/MnO <sub>2</sub>	2 hours	46.01	0.457	33.10 nm
4.	Pure MnO <sub>2</sub> NPs	2 hours	45.87	0.35	42.56 nm

From above table it can be investigated that the crystallite size goes on decreases with rise of ZnO concentration in MnO<sub>2</sub>.

### FTIR Spectrum Analysis

The FTIR electromagnetic spectrum of synthesized specimen of ZnO(5%, 10% and 20%) doped MnO<sub>2</sub> nano-sized stuff ignited at 600<sup>0</sup>C are exhibited for a fixed time duration of 2hrs was performed using a Perkin Elmer instrument at Punjab University located at Chandigarh. The graphical representation of the obtained data is explored in the figure-2.

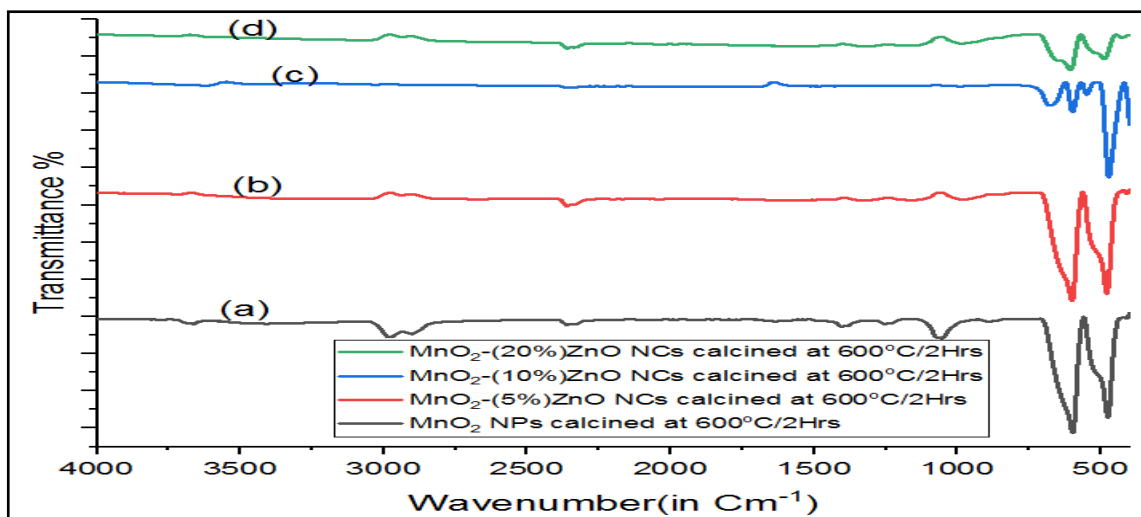


**Figure-2: FTIR Spectra of nano-sized stuff ignited at 600<sup>0</sup>C for 2 hours (a) 5%ZnO /MnO<sub>2</sub> (b) 10% ZnO /MnO<sub>2</sub> (c) 20% ZnO /MnO<sub>2</sub> nano-sized stuff**

The various peaks position of various kind of peak such as Broad band, solder, sharp, minute were observed in spectrograph. The observed peak position was 3402cm<sup>-1</sup>, 2318cm<sup>-1</sup>, 2337cm<sup>-1</sup>, 2330cm<sup>-1</sup>, 837cm<sup>-1</sup>, 516cm<sup>-1</sup>. The peak observed at 3402cm<sup>-1</sup>, 2330cm<sup>-1</sup>, 1546cm<sup>-1</sup> were maybe accredited by presence of water in atmosphere. Whereas sharp alps(peaks) inspected at 598cm<sup>-1</sup> was due to Mn-O-Mn formation and 516cm<sup>-1</sup>, 494 cm<sup>-1</sup> were due to oxide formation of metal i.e., the Alps(peaks) 494 cm<sup>-1</sup> were attributing the Zn-O-Zn vibrations and these Alps(peaks) and therefore, confirmed the presence of ZnO in MnO<sub>2</sub> nano-sized stuff. The IR spectrum analysis of the synthesized Manganese Oxide nanoparticles revealed several characteristic peaks, indicating the presence of various functional groups. At peak positions 471,483,611cm<sup>-1</sup> and 837 cm<sup>-1</sup>, Mn-O-Mn and Zn-O-Zn vibrations were identified. A peak at 1300 cm<sup>-1</sup> corresponds to Zn-O-Zn bonding. Additionally, peaks at 1546 cm<sup>-1</sup>, 2330 cm<sup>-1</sup>, and 3402 cm<sup>-1</sup> indicate the presence of -OH groups. These -OH group vibrations are due to water molecules present in the atmosphere, which interact with the nanoparticles. This detailed analysis helps in understanding the chemical structure and bonding of the synthesized Manganese Oxide nanoparticles.

**M-H Curve data analysis**

In present work the various calcined samples of Zinc(Zn) 5%,10%,20% doped Manganese Oxide nanocrystalline were studied through VSM tool and result were compare with pure Manganese Oxide sampled calcined at 600°C for 2 hrs. The data received from lab CEERI Pilani were represented in various graph .

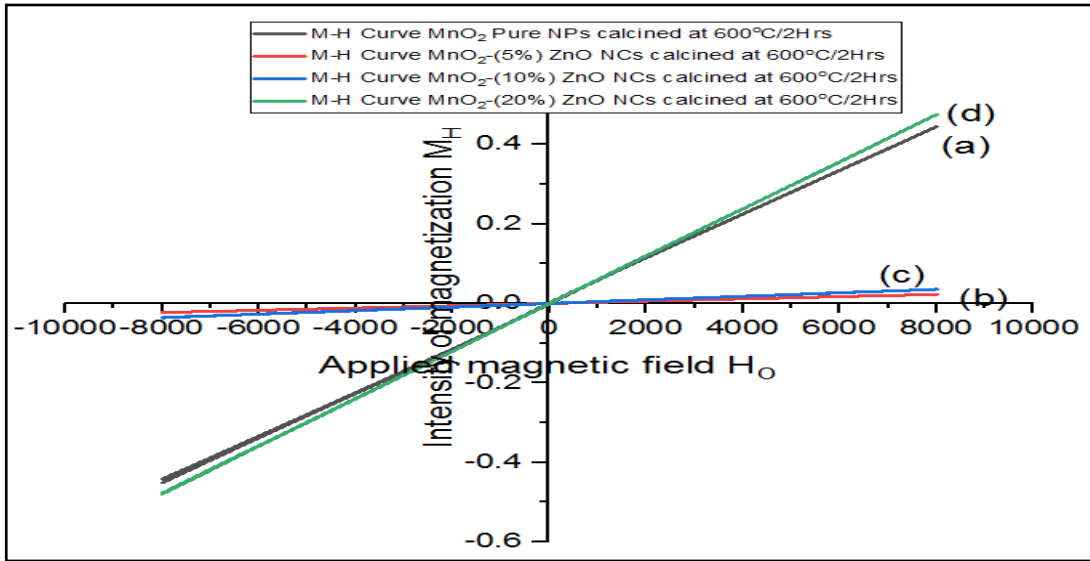


**Figure:3-M-H Curve of pure MnO<sub>2</sub> and Zn (5%, 10%, 20%) doped MnO<sub>2</sub> specimen calcined at 600°C for 2hrs**

The perusal of graphically representation show that the particles are more or less paramagnetic in nature with small hysteresis loss.

**Table 5.2: Magnetic parametric data of pure MnO<sub>2</sub> and Zn (5%, 10%, 20%) doped MnO<sub>2</sub> specimen calcined at 600°C for 2hrs**

Sr . No.	Sample Name	Saturati on Magnetization (10 <sup>-3</sup> emu/g)	Coercive Field (in Hc Oe)	Remanent Magnetization (10 <sup>-3</sup> emu/g)	Squaren ess	Double Square ness Factor	Maximum Permeabilit y (in 10 <sup>-6</sup> emu/g/Oe)	Max. energy loss( in MGsOe)	Sat. field, field (0.95 Ms) X10 <sup>-6</sup> in Hs Oe
1	MnO <sub>2</sub> Pure	447.886	24.97	1.518	0.003	0.035	60.947	447.886	54.924
2	Zn 5%	22.638	31.197	102.024	0.005	0.716	3.291	22.638	2.805
3	Zn 10%	35.725	9.946	46.649	0.001	0.158	4.717	35.725	4.399
4	Zn 20%	477.24	4.916	298.874	0.001	0.604	61.002	475.978	59.707

The above tabular data reflects that saturation magnetization, coercive field, maximum permeability and maximum energy loss continuously reduce with increase of dopant concentration up to concentration level of ZnO 10% doped and thereafter gradually increase saturation magnetization, maximum permeability and maximum energy loss and continuously decrease

coercive field at 20%. It might be due to localized magnetization effect in the crystal because of distortion occurred at higher concentration such as 20%.

#### FESEM images investigations

The scanning of sample through electron microscopy images of ZnO doped MnO<sub>2</sub> nano-sized stuff ignited at 600 °C for 2 hours were more or less similar to typical scanning of sample through electron microscopy [225]. Micrograph of ZnO doped MnO<sub>2</sub> (10%) nano-composites ignited at 600°C for 2 hours is exhibited in **Image 1**

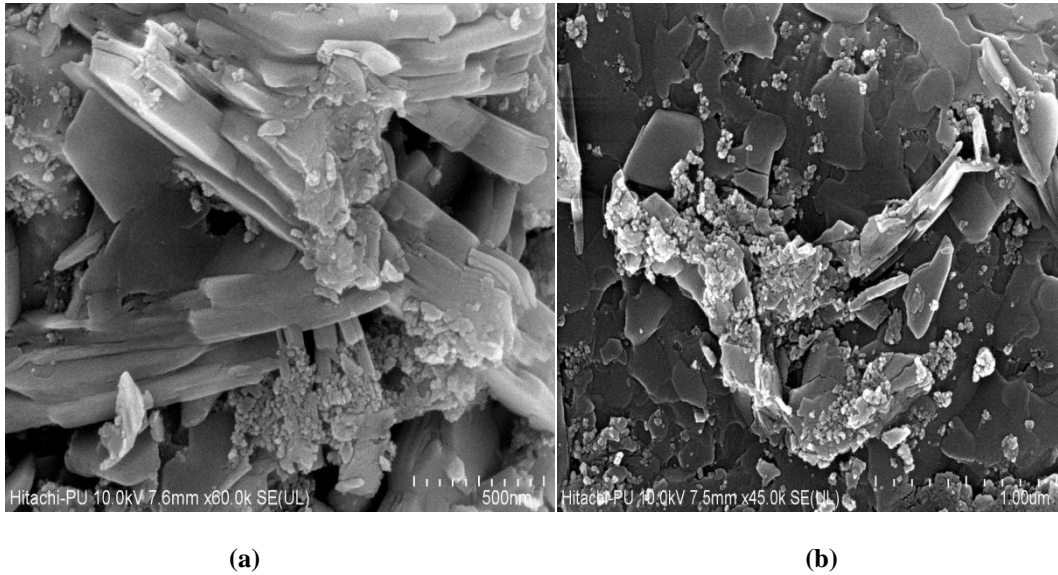


**Figure-4: FESEM image of 10% pure Manganese Oxide nanocrystalline calcined at temperature (a) 400°C (b) 600°C for fixed time interval of two hours.**

Examination of Image exhibits that flecks are polycrystalline, cluttered in style and 2D structure in formation.

#### High-Resolution Transmission Electron Microscope (HRTEM)

HRTEM studies of pure Manganese Oxide nano-particulates which were ignited at 600°C ignition temperature for a fixed time period of 2 hours were done in CIL Lab, Punjab University, Chandigarh and the recorded images were illustrated in the figure below. TEM micro-graphs of ZnO doped MnO<sub>2</sub> nano-composites with various concentrations (5%, 10%, 20%) ignited at 600 °C for 2 hours are exhibited. The images of HRTEM illustrate that the size of prepared pure MnO<sub>2</sub> nanocrystalline is less than 50nm and lies in the nano-regime.

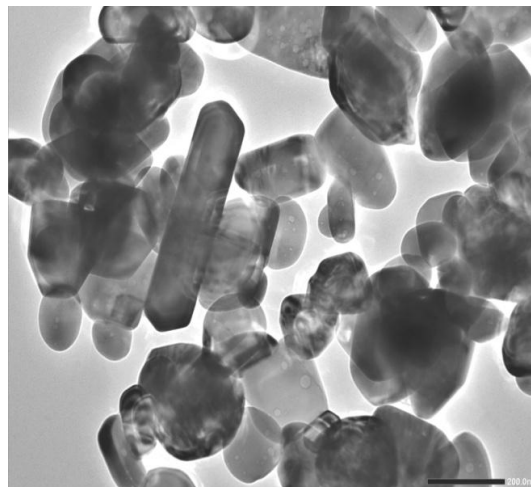


**Figure-5: HRTEM images of ZnO doped MnO<sub>2</sub> (10%) nano-sized stuff ignited at 600 °C for 2 hours**



Examination of the Image exhibits that diameter of the nano-sized stuff ranging from 23.01 to 42.56 nm and intermediate grain size estimated to be 34nm. The micrographs of TEM concluded that grain size results resemble with XRD results and clarified that grain size rises with doping molar concentration. From the micro-graph, it was inspected that the nano-fleck are polycrystalline kind and spherical in contour.

### CONCLUSIONS

The Zinc doped Manganese Oxide nano-crystalline were successfully synthesized by microwave irradiated chemical coprecipitation protocols and XRD results concluded that crystallite size decreases with dopant concentration and crystallite Size of  $\text{MnO}_2$  pure nanoparticulates have maximum size respectively. The FESEM and HRTEM images insure the nanomaterial were 2-D nano-structured and thin film were in formations with different nano range sizes. The IR peaks emphasized that pure Manganese Oxide nanocrystalline were observed with different phase of occurrences. The IR absorption peak results verify the XRD results. The ZnO20% doped  $\text{MnO}_2$  nano-crystallines have superior magnetic properties with compare to other samples and recommended by researchers for applications such as spintronic applications.

**Acknowledgement:**-Authors are thankful to Principal, MNS Government College Bhiwani (Haryana) for providing Lab facility for their synthesis work of samples and also acknowledge their thanks to technical staff, SAIF ,Punjab university Chandigarh to provide lab facility for X Ray diffraction and FESEM of samples and Central Instrumentation Facility (CIF) in Lovely Professional University for the FTIR analysis, Analytical CSIR lab of CEERI Pilani (Rajasthan) for providing results of Vibrating Sample Magnetometer facility for magnetic properties measurements.

### REFERENCES

- [1]. Agrawal, S., Parveen, A. and Azam, A. (2016) 'Influence of mg on structural, electrical and magnetic properties of  $\text{CuAlO}_2$  nanoparticles', Materials Letters, 168, pp. 125–128. doi:10.1016/j.matlet.2016.01.046.
- [2]. Amol Kulkarni, "Amazon Redshift: Performance Tuning and Optimization," International Journal of Computer Trends and Technology, vol. 71, no. 2, pp. 40-44, 2023. Crossref, <https://doi.org/10.14445/22312803/IJCTT-V71I2P107>
- [3]. Sandeep Reddy Narani , Madan Mohan Tito Ayyalasomayajula , SathishkumarChintala, "Strategies For Migrating Large, Mission-Critical Database Workloads To The Cloud", Webology (ISSN: 1735-188X), Volume 15, Number 1, 2018. Available at: [https://www.webology.org/data-cms/articles/20240927073200pmWEBOLBY%2015%20\(1\)%20-%2026.pdf](https://www.webology.org/data-cms/articles/20240927073200pmWEBOLBY%2015%20(1)%20-%2026.pdf)
- [4]. Ahmed, M. et al. (2018) 'Dosimetric properties of CR doped  $\text{Al}_2\text{O}_3$  nanophosphors', Journal of Luminescence, 196, pp. 449–454. doi:10.1016/j.jlumin.2018.01.001.
- [5]. Sheela,Rajesh Sharma & Sunita Dahiya,Modifications in Magnetic properties with Copper Oxide dopant concentration in  $\text{NiCuO}_{2\pm\delta}$  Nanocrystalline,Indian Journal of Pure & Applied Physics Vol.62(2024)1124-1128.
- [6]. Kulkarni, Amol. "Image Recognition and Processing in SAP HANA Using Deep Learning." International Journal of Research and Review Techniques 2.4 (2023): 50-58. Available on: <https://ijrrt.com/index.php/ijrrt/article/view/176>
- [7]. SathishkumarChintala, Sandeep Reddy Narani, Madan Mohan Tito Ayyalasomayajula. (2018). Exploring Serverless Security: Identifying Security Risks and Implementing Best Practices. International Journal of Communication Networks and Information Security (IJCNIS), 10(3). Retrieved from <https://ijcnis.org/index.php/ijcnis/article/view/7543>
- [8]. Sravan Kumar Pala, "Synthesis, characterization and wound healing imitation of  $\text{Fe}_3\text{O}_4$  magnetic nanoparticle grafted by natural products", Texas A&M University - Kingsville ProQuest Dissertations Publishing, 2014. 1572860.Available online at: <https://www.proquest.com/openview/636d984c6e4a07d16be2960caa1f30c2/1?pq-origsite=gscholar&cbl=18750>
- [9]. Credit Risk Modeling with Big Data Analytics: Regulatory Compliance and Data Analytics in Credit Risk Modeling. (2016). International Journal of Transcontinental Discoveries, ISSN: 3006-628X, 3(1), 33-39.Available online at: <https://internationaljournals.org/index.php/ijtd/article/view/97>
- [10]. Nuru-Deen Jaji, Hooi Ling Lee, Mohd Hazwan Hussin, Hazizan Md Akil, Muhammad Razlan Zakaria, and Muhammad Bisyrul Hafi Othman Advanced nickel nanoparticles technology: From synthesis to applications Nanotechnology Reviews 2020; 9: 1456–1480.
- [11]. Banerjee, Dipak Kumar, Ashok Kumar, and Kuldeep Sharma."Artificial Intelligence on Supply Chain for Steel Demand." International Journal of Advanced Engineering Technologies and Innovations 1.04 (2023): 441-449.
- [12]. Abozer Elderderly, Badr Alzahrani, Abdulrahim Alabdulsalam, Synthesis of nickel cobalt-codoped Tin oxide nanoparticles from Psidium guajava with anticancer properties, Arabian Journal of Chemistry (2023) 16, 104481.

- [13]. P. M. Ponnusamy, S. Agilan, N. Muthukumarasamy, M. Raja, Dhayalan Velauthapilla, Studies on cobalt doped NiO nanoparticles prepared by simple chemical method, *J Mater Sci: Mater Electron*.
- [14]. Parikh, H., Patel, M., Patel, H., & Dave, G. (2023). Assessing diatom distribution in Cambay Basin, Western Arabian Sea: impacts of oil spillage and chemical variables. *Environmental Monitoring and Assessment*, 195(8), 993
- [15]. Goswami, MaloyJyoti. "Leveraging AI for Cost Efficiency and Optimized Cloud Resource Management." *International Journal of New Media Studies: International Peer Reviewed Scholarly Indexed Journal* 7.1 (2020): 21-27.
- [16]. Goswami, MaloyJyoti. "Study on Implementing AI for Predictive Maintenance in Software Releases." *International Journal of Research Radicals in Multidisciplinary Fields*, ISSN: 2960-043X 1.2 (2022): 93-99.
- [17]. Sravan Kumar Pala, "Implementing Master Data Management on Healthcare Data Tools Like (Data Flux, MDM Informatica and Python)", *IJTD*, vol. 10, no. 1, pp. 35-41, Jun. 2023. Available: <https://internationaljournals.org/index.php/ijtd/article/view/53>
- [18]. Banerjee, Dipak Kumar, Ashok Kumar, and Kuldeep Sharma. Machine learning in the petroleum and gas exploration phase current and future trends. (2022). *International Journal of Business Management and Visuals*, ISSN: 3006-2705, 5(2), 37-40. <https://ijbmv.com/index.php/home/article/view/104>
- [19]. Mohsen Mohammadijoo, S.K. Sadrnezhad, Vahid Mazinani, Synthesis and characterization of nickel oxide nanoparticle with wide band gap energy prepared via thermochemical processing, *Nanoscience and Nanotechnology: An International Journal* 2014; 4(1)6-9.
- [20]. Neha Yadav, Vivek Singh, "Probabilistic Modeling of Workload Patterns for Capacity Planning in Data Center Environments" (2022). *International Journal of Business Management and Visuals*, ISSN: 3006-2705, 5(1), 42-48. <https://ijbmv.com/index.php/home/article/view/73>
- [21]. Vivek Singh, Neha Yadav. (2023). Optimizing Resource Allocation in Containerized Environments with AI-driven Performance Engineering. *International Journal of Research Radicals in Multidisciplinary Fields*, ISSN: 2960-043X, 2(2), 58-69. Retrieved from <https://www.researchradicals.com/index.php/rr/article/view/83>
- [22]. Nagaraj, B., Kalaivani, A., SB, R., Akila, S., Sachdev, H. K., & SK, N. (2023). The Emerging Role of Artificial Intelligence in STEM Higher Education: A Critical review. *International Research Journal of Multidisciplinary Technovation*, 5(5), 1-19.
- [23]. Parikh, H. (2021). Diatom Biosilica as a source of Nanomaterials. *International Journal of All Research Education and Scientific Methods (IJARESM)*, 9(11).
- [24]. Pillai, Sanjaikanth E. VadakkethilSomanathan, et al. "Mental Health in the Tech Industry: Insights From Surveys And NLP Analysis." *Journal of Recent Trends in Computer Science and Engineering (JRTCSE)* 10.2 (2022): 23-34.
- [25]. TS K. Anitha, Bharath Kumar Nagaraj, P. Paramasivan, "Enhancing Clustering Performance with the Rough Set C-Means Algorithm", *FMDB Transactions on Sustainable Computer Letters*, 2023.
- [26]. BK Nagaraj, "Theoretical Framework and Applications of Explainable AI in Epilepsy Diagnosis", *FMDB Transactions on Sustainable Computing Systems*, 14, Vol. 1, No. 3, 2023.
- [27]. Pillai, Sanjaikanth E. VadakkethilSomanathan, et al. "Beyond the Bin: Machine Learning-Driven Waste Management for a Sustainable Future. (2023)." *Journal of Recent Trends in Computer Science and Engineering (JRTCSE)*, 11(1), 16-27. <https://doi.org/10.70589/JRTCSE.2023.1.3>
- [28]. Huanhao Xiao, Shunyu Yao, Hongda Liu, Fengyu Qu, Xu Zhang, Xiang Wu, NiO nanosheet assembles for supercapacitor electrode materials, *Progress in Natural Science: Materials International* 26 (2016) 271-275.
- [29]. Parikh, H. (2021). Algae is an Efficient Source of Biofuel.
- [30]. Bharath Kumar Nagaraj, SivabalaselvamaniDhandapani, "Leveraging Natural Language Processing to Identify Relationships between Two Brain Regions such as Pre-Frontal Cortex and Posterior Cortex", *Science Direct, Neuropsychologia*, 28, 2023.
- [31]. Tanuja Kumari, Sunita Dahiya & Rajesh Sharma, The Calcinations Temperature Dependent structural and optical behaviour of ZnMnO<sub>3-Δ</sub> Nanocrystalline, *Indian Journal of Pure & Applied Physics* Vol. 62(2024) 1113-1117.